PRECISION VECTOR-DIFFERENCE TRANSFORMER WITH HIGH COMMON-MODE REJECTION

F. Cabiati, U. Pogliano, G. C. Bosco

Istituto Elettrotecnico Nazionale Galileo Ferraris,
Strada delle Cacce 91, I-10135 Torino, Italy
Phone (011) 3919435 Fax (011) 346384 e-mail: cabiati@me.ien.it

Abstract – *The problem of obtaining the difference of two AC voltages represented by vectors with arbitrary amplitude and phase at accuracy levels unattainable with electronic amplifiers is addressed. A solution consisting in a precision complex transformer is presented, together with a mathematical model and some preliminary studies of more general interest. A shielded prototype has performed accuracy levels below* 1×10^{-6} *from 30 Hz to 12 kHz and a common-mode rejection ratio exceeding 140 dB from 800 Hz to 40 KHz.*

Keywords - AC difference, common-mode rejection, precision transformer.

1. INTRODUCTION

The problem of differential measurement occurs in many contexts and finds a general solution in electronics, where the differential architecture has become usual for analogue signal processing and related devices. Nevertheless, in the particular field of precision AC measurements, accuracy is limited by the inadequate common-mode rejection and gain accuracy of electronic devices. In fact, they may approach the requirements of measurements in the 10^{-6} accuracy level for very-low frequencies, but in the kilohertz range their behaviour becomes unsatisfactory.

In the present work, the use of a multiple-core transformer is considered, taking advantage of the outstanding features of the ratio transformer with high-permeability core, which constitutes the basic device of many low-frequency measuring systems of high accuracy [1]. Multiple-core transformer devices had already been developed and analysed, both by model and experimental prototype, to obtain improved performance [2] [3].

The context to which the study is referred is that of two AC low frequency voltages, defined at coaxial ports, whose difference is required as available at a coaxial port as well. Such a situation can occur for simple voltage comparison, where the output difference is small compared to the two input voltages, but also for power or impedance measurements, where the input and output voltages are represented by vectors forming a triangle with sides of the same order of magnitude. In particular, the application to an impedance measuring system based on the above principle [4] and already operative is planned.

For applications where the voltage difference is very small relative to each of the voltages, a transformer with the primary winding directly connected between the inner contacts of the two voltage ports is normally used, namely for calibration of inductive voltage dividers. In this particular case, the common-mode voltage sensitivity due to stray capacitance from winding to shield is avoided by introducing a guard shield driven to a voltage very close to the inputs. Such a guarding technique cannot be used when the input voltage difference is large, as the two primary windings would not be at the same potential and then there would not be a unique guard voltage to apply. Thus a solution with independent primary windings individually guarded with shields at ground potential has been considered. Each of these windings produces a strictly proportional magnetic flux and the two fluxes are linked in opposite senses by a secondary winding where the difference voltage is induced.

2. THE DIFFERENCE TRANSFORMER

A conceptual schematic diagram of the vector difference transformer is given in Fig. 1. The two-stage technique is applied to enhance the accuracy of each of the two flux components proportional to the input voltages $\boldsymbol{U}_1$ and $\boldsymbol{U}_2$ respectively, so that the transformer has actually four cores.

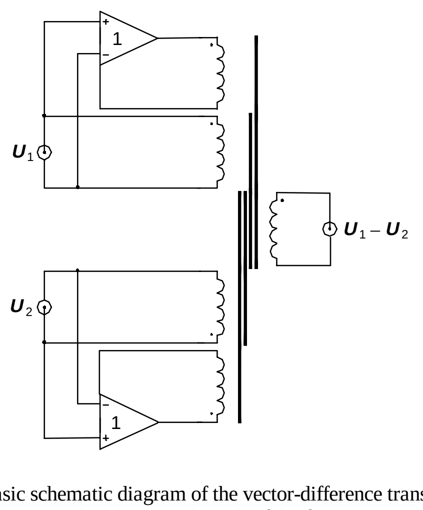

Fig. 1 – Basic schematic diagram of the vector-difference transformer with electric and magnetic shields omitted. Each of the four magnetic cores is linked by the faced winding(s).

In the figure, each winding is conventionally represented as faced to all and only the core(s) that links. The excitation windings, which derive most of the current, are fed by unity-gain boosters to reduce the load at the input voltage ports. The boosters are not necessary where voltages close to $\boldsymbol{U}_1$ and $\boldsymbol{U}_2$ are available, from generators suitable to be loaded, in the same system to which the transformer is applied. This is the case, for example, in impedance comparison systems for four-port standards, where the input voltages of the difference transformer could be applied to the voltage ports on the high sides of the standards, while the excitation currents could be derived from the corresponding current ports.

3. A NETWORK MODEL

The design of the difference transformer can profit by an analysis of the main causes of deviation from the ideal performance. Those related to series and parallel stray parameters of the composite transformer have been determined by means of a mathematical model based on an equivalent circuit, whose schematic diagram is reported in Fig. 2.

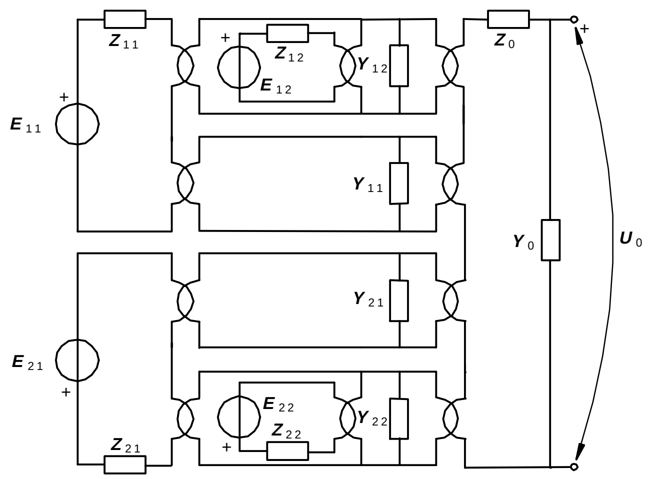

Fig. 2 – Equivalent circuit of the difference transformer based on ideal transformers.

Each magnetic core of the composite transformer is represented by its magnetisation admittance ($\boldsymbol{Y}_m$) and each winding linked with a core by an ideal transformer with the primary derived on $\boldsymbol{Y}_m$. All the parasitic parameters of the windings are represented by series impedances and parallel admittances affecting the secondaries of the ideal transformers. When the secondaries are closed on an ideal voltage generator, the respective parallel admittance is omitted, as it does not significantly affect the operation of the transformer.

The input voltages $\boldsymbol{U}_1$ and $\boldsymbol{U}_2$ of Fig. 1 are represented by $\boldsymbol{E}_{11}$ and $\boldsymbol{E}_{21}$, while $\boldsymbol{E}_{12}$ and $\boldsymbol{E}_{22}$ supply the excitation currents to the first-stage primary windings and may correspond to the outputs of the booster amplifier of Fig. 1 or to some other auxiliary source available within the system, as discussed in section 2.

For the scope of the present analysis, the following equalities can be assumed by symmetry

$$\begin{aligned} &\boldsymbol{Z}_{11} = \boldsymbol{Z}_{21} = \boldsymbol{Z}_1,\ \boldsymbol{Z}_{12} = \boldsymbol{Z}_{22} = \boldsymbol{Z}_2, \\ &\boldsymbol{Y}_{11} = \boldsymbol{Y}_{12} = \boldsymbol{Y}_{21} = \boldsymbol{Y}_{22} = \boldsymbol{Y}_m, \\ &\boldsymbol{E}_{11} = \boldsymbol{E}_{12} = \boldsymbol{E}_1,\ \boldsymbol{E}_{21} = \boldsymbol{E}_{22} = \boldsymbol{E}_2. \end{aligned} \qquad (1)$$

From the complete solution of the system of equations related to the circuit of Fig. 2, a particular solution was considered, as most significant of the deviation from the ideal performance of the difference transformer. It corresponds to the condition $\boldsymbol{U}_2 = 0$, from which the following equalities derive

$$\boldsymbol{E}_{11} = \boldsymbol{E}_{12} = \boldsymbol{U}_1,\ \boldsymbol{E}_{21} = \boldsymbol{E}_{22} = 0. \qquad (2)$$

If the vector relative deviation from the ideal performance is defined as

$$\boldsymbol{\varepsilon} = \frac{\boldsymbol{U}_0 - (\boldsymbol{U}_1 - \boldsymbol{U}_2)}{\frac{1}{2}\left|\boldsymbol{U}_1 + \boldsymbol{U}_2\right|}\ , \qquad (3)$$

then, under (1) and (2) and omitting numerous negligible terms, it results

$$\boldsymbol{\varepsilon} \cong -\boldsymbol{Y}_m^2\, \boldsymbol{Z}_1 \boldsymbol{Z}_2 - \boldsymbol{Y}_0 \boldsymbol{Z}_0 - 2\boldsymbol{Y}_0 \boldsymbol{Z}_1 - 8\boldsymbol{Y}_0 \boldsymbol{Y}_m \boldsymbol{Z}_1 \boldsymbol{Z}_2\,. \qquad (4)$$

Quantitative evaluations of $\boldsymbol{\varepsilon}$ can be obtained by replacing the parameters in (4) with complex functions of frequency and turn number. Actually, such functions have been determined by fitting preliminary experimental data.

The typical frequency behaviour of the conductive and reactive components G_p and $-B_p$ of the parallel-equivalent representation of $\boldsymbol{Y}_m$ related to a Supermalloy toroidal magnetic core are reported in Fig. 3. The values are referred to a conventional 1-turn winding and are intended to be converted for any turn-number n multiplying by $1/n^2$.

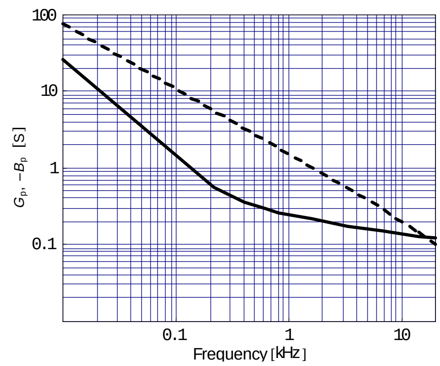

Fig. 3 – Frequency dependence of the conductive component (solid line) and reactive component (dashed line) of the magnetisation admittance in the parallel equivalent representation for a Supermalloy toroidal core. The diagram is referred to a 1-turn winding for generality.

The series impedances show little deviation from linearity, unless for windings that link a magnetic shield. Fig. 4 reports the typical diagrams of the winding series resistance and reactance (lower curves) compared with the same diagrams for a secondary winding over a Mumetal magnetic shield (higher curves). The capacitance of the secondary winding is accounted for by $\boldsymbol{Y}_0$, the only one significantly affecting the accuracy of the transformer, as it is not directly supplied by a generator.

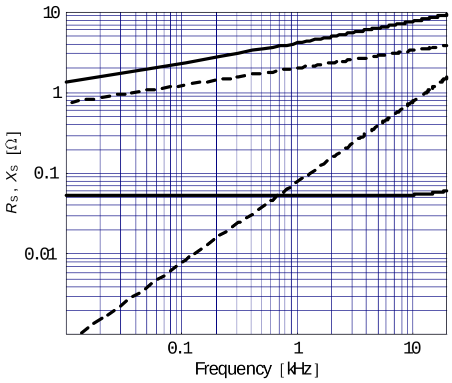

Fig. 4 – Frequency dependence of the series resistance (solid line) and series reactance (dashed line) of a winding of the transformer (lower curves) and of the same winding in case it is wound over a Mumetal magnetic shield (higher curves).

A comprehensive representation of the behaviour of the transformer, useful to the design, is given by the surface plot of the modulus of **ε** as a function of frequency and turn number. Fig. 5 shows such a surface plot as derived from (4) in the case of a single-stage transformer, to point out he adv

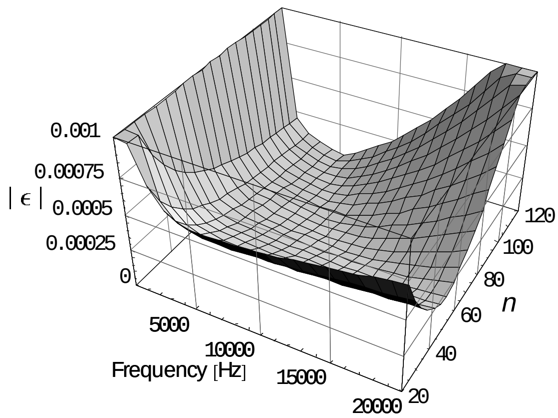

Fig. 5 – Surface plot of the modulus of the relative deviation **ε** from the ideal behaviour of the difference transformer as a function of frequency and turn number for a single-stage configuration.

The behaviour of a single-stage transformer can be obtained from the model based on the diagram of Fig. 2 by imposing, in addition to (1) and (2), also the following conditions

$$\boldsymbol{Z}_{12} = \boldsymbol{Z}_{22} = 0, \quad \boldsymbol{E}_{12} = \boldsymbol{E}_{22} = 0. \tag{5}$$

The improvement due to introduction of the second stage is put in evidence by the plot of Fig. 6, which refers to the configuration of Fig. 1.

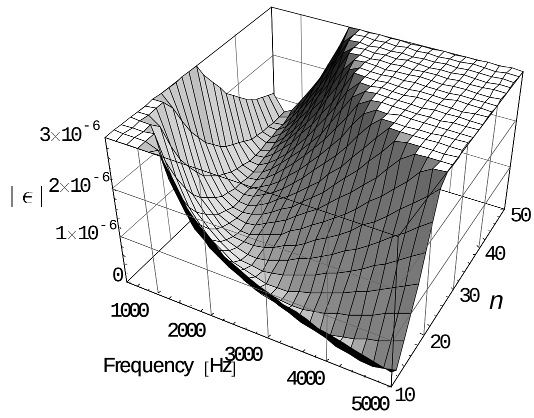

Fig. 6 – Surface plot of the modulus of **ε** as a function of frequency and turn number derived from the mathematical model for the two-stage configura-tion. The improvement compared with the plot of Fig. 5 is evident.

4. THE IMPLEMENTED TRANSFORMER

The main purpose of the research was the improvement of precision impedance measurements, so the design was optimased for the standard frequencies used in this field, that is 1 kHz and 1,592 kHz. Of course, a good behaviour in a range as wide as possible around those frequencies was very appreciated. Therefore, taking into account the plot of Fig. 6, a turn number of 28 was chosen, for which a minimum is shown around the assigned frequency range.

4.1 Shielding Design

The analysis developed on the basis of the network model does not account for the effect of a non uniform distribution of the magnetic flux and imperfect linking between windings and cores. These effects are reduced by means of toroidal shields, which can be of magnetic or conductive material [5]. The magnetic shield is more effective on the low side of the frequency range, while the conductive shield is effective only for frequencies above the kilohertz.

The effectiveness of the shields has been analysed experimentally from a general point of view, before designing the shields of the difference transformer, and it was found that a combination of a Mumetal shield with copper shields should be sufficient to reduce the flux variations along the toroid to a few parts in 10^8 for the chosen turn number of 28. On the other hand, a double conductive shield is also required for a complete capacitive de-coupling of the secondary winding from the primary ones.

While the magnetic shield contributes to the flux uniformity and prevents leakage through the secondary winding, it increases the parasitic series inductance of the secondary winding, as pointed out in Fig. 4, and then the effect of the parallel capacitance and other external loads. For this reason, the magnetic shield was interposed between the excitation winding and the second-stage winding, in order to associate most of its magnetic permeance to that of the second-stage core.

In each of the two symmetrical sections of the difference transformer, two copper shields, each other isolated, were interposed between the second-stage winding and the secondary winding, to be connected to the respective ground terminals.

4.2 Experimental Results

Two series of measurements were carried out on the implemented transformer, with the objective of testing its performance in the most significant input conditions of the large variety of input situations that could be met in practical operation.

One of the conditions ($\boldsymbol{U}_2 = 0$) is the same already considered for the model. In practice, a voltage was applied to both the primary windings of one section of the transformer while those of the other section were put in short circuit. Then the secondary was connected in opposite series with the second-stage primary winding and the residual voltage was analysed by means of a phase-sensitive detector. The results are summarised by the diagrams of Fig. 7, which report the modulus of $\boldsymbol{\varepsilon}$ as defined by (3) and reduced to $\boldsymbol{\varepsilon}_1 = 2\,(\boldsymbol{U}_0 - \boldsymbol{U}_1)\,/\,|\boldsymbol{U}_1|$ in the particular condition. The same diagram is expanded in Fig. 7 (b), to put in evidence the region where $|\boldsymbol{\varepsilon}_1|$ is less than 1×10^{-6}.

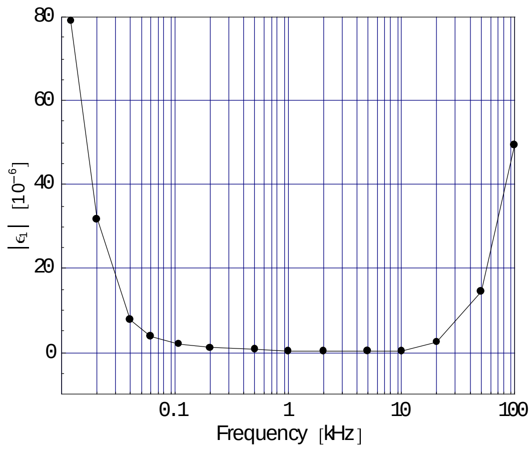

(a)

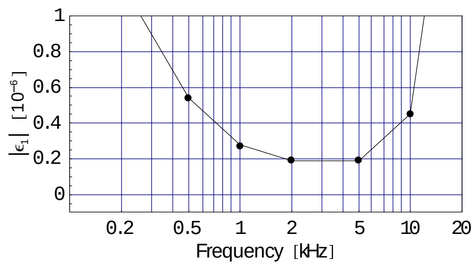

(b)

Fig. 7 – Diagram of the relative deviation $\boldsymbol{\varepsilon}_1 = 2\,|\boldsymbol{U}_0 - \boldsymbol{U}_1|\,/\,|\boldsymbol{U}_1|$ as a function of frequency in a wide range (a) and, with expanded scale, where the deviation does not exceed 1 part in 10^6 (b).

For the other series of measurements, the same voltage was applied to the primary windings of both sections, in order to test the common-mode rejection capability of the difference transformer. The result is expressed by the conventional common-mode rejection ratio (CMRR) as a function of frequency in Fig. 8, where the best specification of an electronic differential amplifier is also reported for reference.

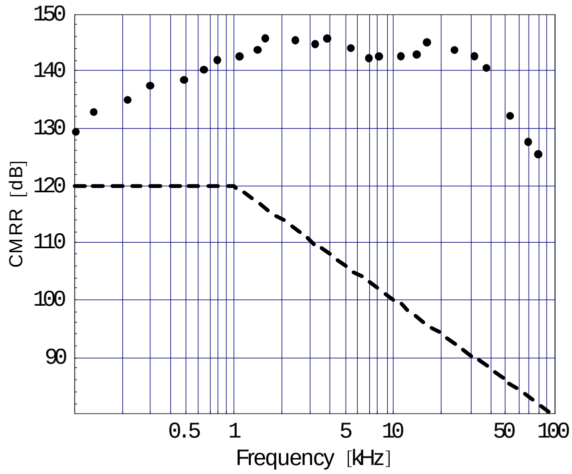

Fig. 7 – Common-mode rejection ratio (CMRR) of the difference transformer. Beside the points corresponding to the measurement data, also the best specification of an electronic differential amplifier is reported (dashed line).

ACKNOWLEDGMENTS

The authors would like to thank D. Serazio and F. Francone for their valid contribution in several preliminary tests and in the construction of the complex transformer.

REFERENCES

[1] B. P. Kibble and G. H. Rayner, *Coaxial AC Bridges*, Adam Hilger, Bristol, 1984, pp. 988-103.

[2] F. Cabiati, G.C. Bosco, “Precision transadmittance amplifier with composite-core isolating transformer”, *Proc. of the 7th IMEKO International Symposium*, Prague, September 1995, pp. 53-57.

[3] F. Cabiati, U. Pogliano, G.C. Bosco, , “An intrinsically compensated three-core current transformer”, *Proc. of the 8th IMEKO International Symposium*, Budapest, September 1996, pp. 13-16.

[4] F. Cabiati, L. Callegaro, A. Muciek, G. C. Bosco, V. D’Elia, ”Generalised impedance comparison with the three-voltmeter method”, *Proc. of the 9th IMEKO International Symposium*, Glasgow, September 1997, pp. 165-168.

[5] G.W. Small, "The efficacy of high permeability and conducting shells as magnetic shields on toroidal cores", *TIP Technical Memorandum No. 144*, CSIRO Telecommunications and Industrial Physics, Australia, 1996.